Research Square

Preprints are preliminary reports that have not undergone peer review.
They should not be considered conclusive, used to inform clinical practice,
or referenced by the media as validated information.

Erdosteine enhances Tobramycin activity in both resistant and sensitive Pseudomonas aeruginosa in vitro and in vivo

Bailey Ramsden
King's College London
Cristina Cigana
IRCCS Ospedale San Raffaele
Davide Gugliandolo
IRCCS Ospedale San Raffaele
Martina Rossano
IRCCS Ospedale San Raffaele
Alessandra Bragonzi
IRCCS Ospedale San Raffaele
Clive Peter Page
King's College London
Richard Thomas Amison
richard.amison@kcl.ac.uk

King's College London

Research Article

Keywords: Pseudomonas aeruginosa, lung infections, erdosteine, tobramycin, antibiotic resistance

Posted Date: July 31st, 2026

DOI: https://doi.org/10.21203/rs.3.rs-10471907/v1

License: This work is licensed under a Creative Commons Attribution 4.0 International License.
Read Full License

Additional Declarations: No competing interests reported.

Abstract

Background

Chronic respiratory infections caused by pathogens including *Pseudomonas aeruginosa* pose a major therapeutic challenge in patients with pulmonary diseases such as cystic fibrosis (CF) and non-CF bronchiectasis, where treatment efficacy is limited by the formation of biofilms, the emergence of multidrug resistant pathogens and a shortage of new and effective antibiotic classes. One approach to address this problem involves the use of “antibiotic enhancers”, which are compounds that potentiate the activity of existing antibiotics without possessing direct antimicrobial effects of their own. The mucoactive thiol-based prodrug erdosteine, currently approved for the treatment of acute and chronic respiratory diseases, has been reported to exhibit anti-adhesive activity against respiratory pathogens, suggesting a clinically relevant contribution to the prevention of bacterial colonization. Furthermore, erdosteine has demonstrated the ability to potentiate the activity of various antimicrobial drugs, but to date has not been investigated for its ability to influence the effect of tobramycin, an antibiotic agent widely used to treat pathogens in the respiratory tract. Furthermore, whilst erdosteine exhibits a wide range of pharmacological actions, including mucolytic, anti-inflammatory, antioxidant activity, the ability to reduce viral load and inhibit bacterial adhesion to epithelial cells, the mechanism of its antibiotic potentiating properties remains poorly understood. In this study, we investigated the ability of MET-1, the primary active metabolite of erdosteine, to enhance the activity of tobramycin against *P. aeruginosa* strains using a panel of both *in vitro* and *in vivo* assays.

Methods

The activity of both mono- and combination therapies was measured in planktonic *P. aeruginosa* (strains RP73 & PA01) using *in vitro* microdilution assays including chequerboard analysis and time-kill assays, whilst activity against biofilms were analysed using microtiter plate assays with readouts including total biomass, metabolic activity, and bacterial enumeration. Combination therapy of 40mg/kg tobramycin and 100mg/kg erdosteine was also assessed *in vivo* using a murine model of chronic pulmonary infection induced by *P. aeruginosa.*

Results

10mg/L MET-1 significantly enhanced the antimicrobial activity of tobramycin in planktonic cultures of RP73 at 24 hrs and PA01 at 4 and 7 hrs, leading to a greater than 2 log reduction in bacterial numbers compared to monotherapy, while MET-1 alone showed no measurable reduction under the same experimental conditions. In biofilm cultures, MET-1 significantly reduced the IC50 of tobramycin in mature RP73 and PA01 biofilms by 15 and 5-fold respectively. Finally, combination therapy of 40mg/kg tobramycin and 100mg/kg erdosteine significantly reduced bacterial load in a murine model of chronic pulmonary infection.

Conclusions

Our *in vitro* and *in vivo* studies highlight the ability of erdosteine to potentiate the activity of tobramycin suggesting that erdosteine has the potential to reduce the burden of long-term antimicrobial therapies in patients with chronic respiratory infections and thus improve clinical outcomes.

Introduction

Chronic respiratory diseases such as chronic obstructive pulmonary disease (COPD), cystic fibrosis (CF), and chronic bronchitis (CB) are often associated with persistent inflammation leading to chronic lung damage, impaired mucociliary clearance and dysregulated immune responses preventing effective pathogen clearance. As a result, these diseases are associated with chronic bacterial colonisation of the small airways by pathogens of the *Staphylococcus* and *Pseudomonas* genera (1). Furthermore, these patients are also associated with frequent acute infective pulmonary exacerbations (PEx), which are known to be a primary cause behind accelerated lung function decline and disease severity (2–4). Treatment of these chronic infections is limited by the formation of bacterial biofilms, where the formation of extracellular matrix structures associated with mature biofilms shields pathogens from both host immune responses and limits the penetration and activity of conventional antimicrobial therapies (5, 6). Treatment is further complicated by the rise of multidrug-resistant (MDR) and extensively drug-resistant (XDR) pathogens (7–10).

Tobramycin remains a primary therapy for *Pseudomonas aeruginosa* (*P. aeruginosa*) infections, administered as an inhaled formulation for chronic infections (11) or intravenously for acute exacerbations. However, the growing prevalence of tobramycin-resistant *P. aeruginosa* strains, coupled with the limited availability of novel antibiotic classes, has made these infections increasingly challenging to manage. One approach to overcome bacterial resistance has focused on adjunctive therapies that can enhance or restore antimicrobial activity of existing antibiotics.

The orally active thiol-derived pro-drug erdosteine is a licenced medicine used internationally to treat acute and chronic respiratory diseases, including acute episodes of bronchitis. Whilst originally licenced as a mucolytic, there is both pre-clinical and clinical evidence for a multimodal mechanism of action for erdosteine including mucoactive, antioxidant, anti-inflammatory, antiviral and antibiotic enhancing activities (12–14). Significant therapeutic benefits of erdosteine have been reported, with its use as adjunct therapy reducing mucus production, sputum viscosity, and reactive oxygen species (ROS) leading to reduced dyspnoea and increased FEV1 in patients with COPD and CB (15–17). Significantly, multiple clinical studies have now demonstrated that chronic erdosteine therapy reduces both duration and frequency of PEx (18–21).

One previous concern for the use of thiol-derived mucolytic agents, particularly carbocysteine and N-acetylcysteine (NAC), is their potential to interact with multiple classes of antibiotics, leading to reduced antimicrobial activity through drug–drug interactions (22). However, structural differences between

erdosteine and the other thiol-derivatives appear to remove this negative interaction. Indeed, rather than compromising activity, erdosteine has demonstrated numerous antibiotic-enhancing capabilities. *In vitro* studies using the active metabolite N-thiodiglycolyl-homocysteine (MET-1) have demonstrated reduced bacterial adhesion to lung epithelial cells and improved antimicrobial activity of vancomycin, linezolid, amoxicillin and levofloxacin in *Staphylococcus aureus* (*S. aureus*) biofilms through enhanced drug penetration. In fact, erdosteine has been shown to possess anti-adhesive properties, as demonstrated by Braga et al. with evidence of reduced bacterial adherence to epithelial cells, supporting a potential role in limiting colonization and infection (23–25). Importantly, this has also been reported clinically through enhanced clinical activity of amoxicillin in CB patients. A meta-analysis of 7 randomised clinical trials (RCTs) revealed that erdosteine plus antibiotics was more effective than antibiotic monotherapy in patients with CB/COPD for the treatment of acute infective PEx (26, 27). However, despite the ability of erdosteine to improve the activity of different classes of antibiotics against gram-positive pathogens such as *S. aureus* (25), its ability to potentiate standard-of-care (SoC) antibiotic therapy against gram-negative pathogens such as *P. aeruginosa*, which typically cause respiratory infections, has not been explored. We therefore set out to investigate the potential benefits of erdosteine in combination with tobramycin against two *P. aeruginosa* isolates: (1.) RP73, a MDR clinical isolate associated with chronic infections (28), and (2.) PA01, a well-characterised laboratory reference strain commonly used to study pathogenesis and biofilm formation (29). We combined conventional *in vitro* assays of bactericidal activity such as the chequerboard assay of synergy, bacterial time-kill and biofilm microtiter assays coupled with an *in vivo* murine model of chronic pulmonary infection.

Materials and Methods

In vitro bacterial culture conditions and maintenance.

All bacterial strains were stored at -80°C using the CryoBead system and routinely maintained using Tryptone Soy Agar (TSA). Two *P. aeruginosa* strains were provided by Dr Alessandra Bragonzi at the Infection and Cystic Fibrosis Unit, San Raffaele Scientific Institute, Milan, Italy. The fully sequenced tobramycin-sensitive laboratory reference strain, PA01, and a multi-drug resistant non-mucoid strain, RP73, isolated 17.5 years post onset of infection in a CF patient (28, 29). For chequerboard and time-kill assays, bacteria were grown in tryptic soy broth (TSB), whilst in biofilm studies TSB was supplemented with glucose and NaCl to promote biofilm formation. For *in vivo* studies, RP73 was grown on TSA and cultured in nutrient broth at 37°C, 120 rpm.

Drug preparation.

Erdosteine and its primary active metabolite, MET-1, were kindly donated by Edmond Pharma (Milan, Italy). MET-1 and erdosteine were dissolved in 100% DMSO (10 g/L) and working stock solutions (1 g/L) prepared by the addition of PBS prior to sterilisation by filtration at 0.20µm (Cambridge Bioscience Ltd., Cambridge, UK). For *in vivo* studies, erdosteine was dissolved in DMEM and adjusted to pH 6.8.

Tobramycin (Fisher Scientific) stocks were prepared in PBS at 1 g/L and filter sterilised (0.22µm). All stock solutions were stored at -20°C and were single-use once thawed.

Minimum Inhibitory Concentration (MIC) assay.

MET-1, erdosteine and tobramycin MICs were calculated for RP73 and PA01. MICs were determined at the growth/no-growth interface following EUCAST methodology as previously reported (30). Briefly, serial 2-fold dilutions of the drug were prepared in TSB in flat-well polycarbonate 96 well plates and treated with $5x10^6$ cfu/100µL. Plates were sealed with a breathable membrane and incubated in a humidified chamber at 37°C for 16–20 hours. Resazurin sodium salt was added to a final concentration of 0.15 mM and plates were incubated for an additional 2–4 hours. Resazurin is a blue-coloured dye that is reduced by aerobic respiration of metabolically active cells to the pink-coloured fluorescent resorufin (30, 31).

Chequerboard Assay of Synergy.

As erdosteine is a prodrug, for all *in vitro* efficacy assays, we used the primary active metabolite MET-1. MET-1-tobramycin combinations were prepared in TSB in 96-well plates. The starting concentration for tobramycin was 2x MIC and, given that no MIC could be determined for MET-1, the highest soluble concentration of MET-1 was used (1024 mg/L). A double serial 2-fold dilution of each drug in PBS was then performed in sterile flat well polycarbonate plates creating a total of 64 different combinations per pair. Plates were sealed with a breathable membrane and incubated in a humidified chamber at 37°C for 16–20 hours. Resazurin sodium salt was added to a final concentration of 0.15 mM and plates were incubated for an additional 2–4 hours. Given the lack of MIC for MET-1, the Fractional Inhibitory Concentration Indices (FICI) could not be calculated. Instead, the effect of the combination was determined based on the difference between the MIC of tobramycin as a monotherapy and in combination with MET-1 using a growth/no-growth interface.

Bacterial Time-Kill Assays.

RP73 or PA01 at $5x10^5$ cfu/mL were cultured in the presence of vehicle, tobramycin, MET-1 (10 mg/L), or tobramycin in combination with either 2, 5 or 10 mg/L MET-1. MET-1 was used at concentrations in the same order of magnitude of the blood peaks obtainable at the common therapeutic doses (23, 24). Tobramycin was used at concentrations 0.5, 1 and 4 times the MIC as determined by the methodology described above. Bacterial viability was determined by aliquot collection at 0, 2-, 4-, 7- and 24-hours post-inoculation. Samples of bacterial suspensions were serially diluted in sterile PBS and plated on TSA for bacterial enumeration following overnight incubation.

Biofilm Microtiter Assays.

Effects on Biofilm formation

Colonies of either RP73 or PA01 were inoculated in TSB and cultured for 18–20 hours at 37°C (130 rpm). After incubation, bacterial cultures were centrifuged at 4500g at 4°C for 10 minutes and the pellet washed in PBS. To investigate the effect of MET-1 on growing biofilms, $1x10^7$ cfu/mL were treated with either vehicle control (PBS), MET-1 (2, 5 and 10mg/L), or MET-1 in the presence of tobramycin (4x MIC) and allowed to develop as biofilms in a sterile flat well polycarbonate 96-well plate (200µL/well). Plates were sealed with a breathable membrane and incubated in a humidified chamber at 37°C for 6, 24 or 48 hours under static conditions.

Effects on Established Biofilms

200µL of $1x10^7$ cfu/mL were added to sterile flat well polycarbonate 96-well plates, sealed with a breathable membrane and incubated in a humidified chamber at 37°C. To enable detailed analysis of biofilm eradication a concentration-response curve was created for tobramycin mediated biofilm eradication using 0, 0.25, 0.5, 1, 5, 20, 50, 100, 200, 400 and 800x MIC tobramycin. To investigate the potentiating capabilities of MET-1, at 6, 24 or 48 hours of biofilm growth, media was carefully removed and replaced with TSB supplemented with either vehicle (PBS), tobramycin (0-800x MIC), MET-1 (2, 5, 10mg/L) or combinations thereof. Plates were sealed with a breathable membrane and incubated in a humidified chamber at 37°C for a further 24 hours. After 24 hours, biofilm eradication was quantified as either changes in biomass, metabolic activity or absolute colony-forming units (cfu) quantification within biofilms.

Biofilm Biomass Quantification.

Biofilm biomass was determined through absorbance at 570nm of crystal violet (CV) staining as previously described (25). At each biofilm incubation timepoint, media was removed, and biofilms were carefully washed three times with PBS to remove any non-biofilm resident bacteria. Biofilms were fixed by heat at 60°C for 1 hour on a hot plate and stained for 15 minutes with 150µL of 2.3% CV in 20% ethanol at room temperature. After staining, excess CV was removed and the biofilm washed three times with PBS. Wells were air-dried, and biofilm bound CV resolubilized with 200µL of 33% (v/v) glacial acetic acid for 1 hour at room temperature. Contents of wells were transferred to a new plate and CV absorbance was measured at 570 nm using a microplate spectrophotometer with 33% acetic acid in water as a blank.

Bacterial Metabolic Activity Quantification.

Metabolic activity of all biofilm-associated bacteria was determined using resazurin. At each biofilm incubation timepoint, media was removed and the biofilms were washed three times with sterile PBS to remove any non-biofilm resident bacteria. Biofilms and sterility controls (TSB only) were incubated with 10µg/mL resazurin in TSB until the control wells sufficiently turned pink (1–6 hours depending on the strain and biofilm age). Resorufin fluorescence was measured at a wavelength of 590 nm with excitation wavelength of 550 nm.

Bacterial Viability of Biofilm-associated Bacteria.

Bacterial burden within biofilms was assessed by quantifying cfu using agar plating. At each time point, media was removed and the biofilms washed three times with PBS to remove any non-biofilm resident bacteria. 200µL of sterile PBS was added to each well and the plate was sealed. Biofilms were removed from the wells using sonication for 3 minutes at high intensity as previously reported (31). Aliquots were serially diluted with sterile PBS and plated onto TSA plates. Plates were subsequently incubated at 37°C for 16–18 hours, and cfu counted.

Murine Model of Pulmonary Infection

Monotherapies of tobramycin, erdosteine or combinations thereof were assessed using a murine model of chronic pulmonary infection with *P. aeruginosa* as previously described (31, 32). All procedures were performed in accordance with protocols approved by the Ospedale San Raffaele Institutional Animal Care and Use Committee (IACUC) and in compliance with Italian Ministry of Health guidelines for the care and use of experimental animals. Immunocompetent C57BL/6 NCrlBR mice (8–10 weeks, Charles River Laboratories, Calco, Italy) were challenged with $1x10^6$ cfu/mouse of RP73 embedded in agar beads by intratracheal administration. Mice were treated daily with either vehicle control, 40 or 160mg/kg tobramycin via subcutaneous administration as previously reported (32), 100mg/kg erdosteine via oral gavage (*p.o*), or combinations of tobramycin: erdosteine at 40:100mg/kg, respectively. 10 days post infection, animals were euthanised and a bronchoalveolar lavage (BAL) performed and lungs collected for cfu quantification. Bacterial burden was assessed in both lung homogenates and BAL fluid via plating on TSA plates for quantification of pulmonary bacterial load.

Data Presentation and Analysis.

Data and statistical analysis were performed with GraphPad Prism (GraphPad Software, Inc, San Diego, CA, USA). MIC values are presented as modal values of three repeats performed in triplicate. Time-kill analyses of data between 0–24 hours are presented as log mean cfu/mL ± standard error of the mean (SEM). A log fold reduction of ≥ 2 between monotherapy and combination therapy was determined as synergistic as previously reported (33). Secondary analysis of synergy in bacterial time-kill assays was performed using the BLUR model of synergy (34). Additionally, timepoints of interest were presented as a bar chart, where significant differences between tobramycin monotherapy vs combination treatment groups were assessed using an ordinary one-way ANOVA followed by Tukey's test (ns, $P > 0.05$; * $P \leq 0.05$; ** $P \leq 0.01$; *** $P \leq 0.001$; and **** $P \leq 0.0001$). The limit of detection (LOD) of the time-kill assay was found to be 2 log10 cfu/mL (100 cfu/mL) as previously reported (30).

Biofilm biomass and metabolic activity are expressed as a percentage of the control to account for inherent variability in biofilm growth between cultures (25). Significant differences in biofilm biomass or metabolic activity after 6, 24 and 48 hours were determined using an ordinary two-way ANOVA followed by Tukey's test (ns, $P > 0.05$; * $P \leq 0.05$; ** $P \leq 0.01$; *** $P \leq 0.001$; and **** $P \leq 0.0001$). The minimum reliable signal (MRS), which is the smallest signal level that can be distinguished from background noise

with acceptable accuracy and confidence, was 0.17 (OD570 nm) and 5719 RFU for the crystal violet and resazurin assay, respectively. MRS was calculated using the following equation:

$$\bar{B} + 3\sigma$$

$\bar{B}$ =mean blank absorbance, **σ** = standard deviation of blanks

For *in vivo* studies data are presented as mean ± SEM. Normal distribution of data was confirmed using the Shapiro-Wilks normality test and subsequently analysed using a parametric one-way ANOVA followed by the Sidaks multiple comparison post-test.

Results

MET-1 does not affect growth/no-growth threshold in the MIC assay.

MIC values for tobramycin alone and in combination for RP73 and PA01 are shown in **Table 1**. Based on a clinical breakpoint for tobramycin of 2mg/L (35), RP73 is classified as tobramycin-resistant (4mg/L) and PA01 tobramycin-sensitive (1mg/L). Combination with MET-1 did not show any change in tobramycin MIC for either of the *P. aeruginosa* strains, RP73 or PA01. In line with previous work, MET-1 monotherapy did not achieve a growth/no-growth threshold in the MIC assay at the highest soluble concentration of MET-1 (1024 mg/L). As MET-1 does not achieve a growth/no growth interface, it was not possible to calculate any FICI values for tobramycin in the presence of MET-1 and therefore no additive/synergistic interactions were detected using the chequerboard assay of synergy.

MET-1 potentiates tobramycin against planktonic RP73 and PA01 *in vitro*.

Combinations of tobramycin and MET-1 were assessed in a bacterial time-kill assay, as this approach captures dynamic changes in bacterial viability over time. We analysed the ability of 10mg/L MET-1 to potentiate the antimicrobial activity of tobramycin at 0.5x, 1x, and 4x MIC for both RP73 (Fig. 1A-C) and PA01 (Fig. 1D-F). The concentration of MET-1 used (10mg/L) is within the same order of magnitude as the plasma peak levels achievable after standard therapeutic dosing of erdosteine. MET-1 exhibited no bactericidal activity against planktonic cultures of RP73 or PAO1, as evidenced by the absence of any significant differences between the untreated control and MET-1 monotherapy at 24 hours. Furthermore, no potentiation of tobramycin was observed with MET-1 at sub-therapeutic antibiotic concentrations (0.5x MIC, Fig. 1A). However, MET-1 (10mg/L) significantly potentiated the activity of tobramycin at 1x and 4x MIC against RP73 at 24 hours, resulting in a log-order reduction in bacterial cells of 4.06 ± 1.57 cfu/ml (Fig. 1B, $P < 0.05$) and 3.85 ± 0.97 cfu/mL (Fig. 1C, $P < 0.05$), respectively, compared to tobramycin alone. Synergy for both tobramycin concentrations was confirmed by secondary BLUR analysis ($P < 0.05$). For PA01 similarly to RP73, no potentiation was observed at 0.5x MIC (Fig. 1D), whilst MET-1 (10mg/L) significantly potentiated the activity of tobramycin at both 1x and 4x MIC at 4 and 7 hours, respectively, with a log-order reduction of 2.05 ± 1.18 CFU/mL at 1x MIC (Fig. 1E, $P < 0.05$) and 3.72 ±

0.79 cfu/mL at 4x MIC (Fig. 1F, $P < 0.05$) compared to tobramycin alone, whilst this effect was lost at 24 hours. Secondary BLUR analysis revealed additive interactions at 1x MIC and synergistic interactions at 4x MIC ($P < 0.05$).

MET-1 delays biofilm formation *in vitro*.

Early biofilm formation represents a clinically important window during which antimicrobial intervention may prevent the transition to persistent, treatment-refractory infections. Given the observed potentiation by MET-1 in planktonic cultures, we next evaluated the impact of MET-1 on biofilm resident cultures. In agreement with previous research indicating that MET-1 can reduce bacterial adhesion, we demonstrated that treatment with MET-1 significantly reduced biofilm biomass for three different *S. aureus* strains (USA300, ATCC33591 and ATCC25923) at 6 hours supporting the concept that MET-1 may be reducing early biofilm development through reduced bacterial adhesion (Supplementary Figs. 1A-C). The response differed in the gram-negative *P aeruginosa* strains RP73 and PA01, in which biofilm biomass was not significantly altered (Supplementary Fig. 1D &E).

We next investigated whether combining tobramycin with MET-1 (2, 5 and 10mg/L) could alter biofilm formation. At 6 or 24 hours of development, no significant difference was observed in either biofilm biomass or metabolic activity of RP73 biofilms grown in the presence of 4x MIC tobramycin monotherapy, or those combined with MET-1 at any tested concentration (Fig. 2A & B). In young biofilms (6 hours) total recovered bacterial numbers were significantly reduced, with log-order reductions in cfu/mL of 1.64 ± 0.28 ($P < 0.05$), 1.65 ± 0.31 ($P < 0.05$), and 1.63 ± 0.24 ($P < 0.05$) for 2, 5 and 10mg/L MET-1 respectively (Fig. 2A). However, this reduction was not seen at 24 hours (Fig. 2B), potentially indicating delayed biofilm formation through reduced bacterial adhesion. Similarly, for PA01 biofilms, no significant differences were seen for biofilm biomass for biofilms grown in the presence of tobramycin (4x MIC) compared to those grown in the presence of tobramycin (4x MIC) in combination with MET-1 (2, 5 and 10mg/L) at either 6 or 24 hours. However, PA01 biofilms treated with 4x MIC tobramycin and MET-1 revealed a significant reduction in metabolic activity at 24 hours compared to tobramycin alone: 44.6% ±8.0% ($P < 0.01$), 46.1%±8.4% ($P < 0.01$), 46.6%±8.7% ($P < 0.01$) for 2, 5 and 10mg/L, respectively. Whilst metabolic activity was reduced at 24 hours, this was not reflected by any changes in bacterial content within the biofilms (Fig. 2D). This suggests that tobramycin:MET-1 combination therapy may delay the formation of biofilms, although there is no evidence for potentiation in tobramycin mediated reduction in *P. aeruginosa* bacterial burden within the biofilm.

MET-1 potentiates tobramycin against established biofilms of PA01 and RP73.

Whilst it was of interest to investigate the potential of MET-1 to synergise with tobramycin in interfering with biofilm formation, greater clinical relevance lies in the ability to disrupt established biofilms, as bacterial cells are more resistant to conventional antibiotics in established mature biofilms. Using readouts of biofilm size (biomass) and viability (metabolic activity), we characterised a concentration response for tobramycin covering 0-800x MIC for antimicrobial activity against RP73 and PA01 biofilms established for 6, 24 and 48 hours prior to drug treatment. We then evaluated the ability of 2, 5 and

10mg/L MET-1 to induce a leftward shift in tobramycin's concentration response curve as measured by reductions in the concentration of tobramycin required to reduce biofilm size/viability by 50% (Log IC50).

In line with previous research, we confirmed that biofilm maturation was associated with significant increases in biofilm biomass in mature (24, and 48 hours) compared to young biofilms (6hrs) for both RP73 (6hrs: 3.80 ± 0.20; 24hrs: 7.29 ± 0.12, $P < 0.001$; 48hrs: 5.77 ± 0.27 OD, $P < 0.001$, Fig. 3A) and PA01 (6hrs: 5.59 ± 0.13; 24hrs: 7.10 ± 0.07, $P < 0.001$; 48hrs: 7.10 ± 0.24 OD, $P < 0.001$, Fig. 3A**)**. This was also reflected with corresponding increases in metabolic activity (data not shown). As increased biofilm maturation is associated with decreased antibiotic efficacy, we next assessed the susceptibility of young and mature biofilms to tobramycin.

Young RP73 biofilms were more susceptible to tobramycin therapy compared to mature biofilms with significant increases in the IC50 for tobramycin at 24 and 48 hours compared to 6 hours for biomass (6hrs: 23.75 ± 1.83 mg/L; 24hrs: 74.53 ± 20.32 mg/L, $P < 0.05$; 48hrs: 86.94 ± 38.45 mg/L, $P < 0.01$, Fig. 3B). Similarly, tobramycin IC50 values were significantly elevated in mature 48 hour PA01 biofilms compared to young 6 hour biofilms for biomass (6hrs: 4.32 ± 0.24 mg/L; 24hrs: 14.42 ± 5.57 mg/L; 48 hours: 16.38 ± 4.41 mg/L, $P < 0.05$, Fig. 3B).This is consistent with previous literature which demonstrated reduced antimicrobial penetration in established biofilms due to increased production of extracellular polymeric substance matrix.

Combination of tobramycin with 2, 5 or 10mg/L MET-1 in mature biofilms (48 hours) induced a statistically significant concentration dependent decrease in the Log IC50 for tobramycin, which was seen in both biofilm biomass (RP73: Veh 1.34 ± 0.10 vs 10mg/L MET-1: 0.08 ± 0.14 LogIC50, $P < 0.0001$; PA01: Veh 1.37 ± 0.26 vs 10mg/L MET-1: 0.26 ± 0.18 LogIC50, $P < 0.001$) and metabolic activity (RP73: Veh 1.62 ± 0.18 vs 10mg/L MET-1: 0.37 ± 0.12 LogIC50, $P < 0.01$; PA01: Veh 1.36 ± 0.05 vs 10mg/L MET-1: 0.39 ± 0.14 Log IC50, $P < 0.001$, Fig. 4). For both RP73 and PA01, this was not seen at 6 hours.

MET-1 potentiates tobramycin in a murine model of chronic RP73 infection.

Having identified that combining MET-1 with tobramycin enhances antimicrobial activity in both planktonic cultures and established biofilms, we advanced our drug combination to an established murine model of chronic infection with *P. aeruginosa* strain RP73. (31, 32, 36). Mice were infected with $1x10^6$ cfu/mouse embedded in agar beads and monitored for 10 days. After infection, animals were treated daily with either vehicle control, 100mg/kg erdosteine via oral gavage, 40 or 160mg/kg tobramycin *s.c.* or combinations thereof. Infection with RP73 established a stable infection that lasted for the duration of the experiment (Day 10: 3.98 ± 0.23 Log cfu/lung, Fig. 5A). Treatment with 160mg/kg tobramycin resulted in complete bacterial clearance by Day 10. In line with our *in vitro* findings, erdosteine showed limited activity as a monotherapy with no significant reduction in bacterial load compared to vehicle control observed following 100mg/kg erdosteine therapy (Veh: 3.98 ± 0.23 vs 100mg/kg ERD: 2.69 ± 0.72 log cfu/lung, Fig. 5A). Monotherapy with sub-threshold concentrations of tobramycin (40mg/kg) demonstrated mild reductions in bacterial load, but again this was not statistically significant when compared to vehicle treated controls (Veh: 3.98 ± 0.23 vs 40mg/kg TOB:

3.40 ± 0.35 log cfu/lung, Fig. 5A). However, when animals were treated with a combination of both 100mg/kg erdosteine and 40mg/kg tobramycin, a significant reduction in pulmonary bacterial load was observed compared to vehicle controls (Veh: 3.98 ± 0.23 vs Combination: 1.53 ± 0.95, $P < 0.05$, Fig. 5A).

Supporting the greater activity observed with combination treatment, we next evaluated the percentage of infected animals that demonstrated complete bacterial clearance in each group shown in Fig. 5B. As expected, vehicle treated animals showed minimal bacterial clearance with 85% remaining chronically infected throughout the duration of the study, whilst treatment with 160mg/kg tobramycin demonstrated 100% clearance. 57% and 33% of animals completely cleared bacterial infection following monotherapy with 100mg/kg erdosteine or 40mg/kg tobramycin respectively, whilst in comparison following combination therapy, 75% of treated animals completely cleared the pulmonary infection (Fig. 5B).

In summary, all these data support our *in vitro* findings demonstrating an ability of erdosteine to significantly potentiate the antimicrobial activity of tobramycin in a murine model of chronic infection with *P. aeruginosa*.

Discussion

Lower respiratory tract infections with gram-negative pathogens such as *P. aeruginosa* are one of the leading causes of death globally and have a particular impact on patients with chronic respiratory diseases such as CF and COPD, where accumulation of hyper concentrated mucus in the airways facilitates biofilm formation and reduces antibiotic activity (37). Therefore, drugs that improve antibiotic penetration or potentiate antimicrobial activity may offer a valuable strategy to enhance treatment outcomes. The orally active prodrug erdosteine, originally developed as a mucolytic for the treatment of acute and chronic respiratory diseases, has demonstrated pre-clinical and clinical evidence of a multimodal mechanism of action, including mucoactive, antioxidant, anti-inflammatory and antiviral actions (12, 13). Furthermore, unlike other thiol-based mucolytics such as carbocysteine and N-acetylcysteine which have been shown to inactivate antibiotics, due to the unique chemical structure of erdosteine, research has demonstrated antibiotic-enhancing activities against Gram-positive pathogens (12, 13, 25, 26). Here we provide evidence that erdosteine also enhances the aminoglycoside antibiotic tobramycin against both drug-sensitive and drug-resistant strains of *P. aeruginosa*.

Whilst *P. aeruginosa* biofilms present a unique clinical challenge, as they are derived from planktonic precursor populations, assessing antimicrobial combinations against both planktonic and biofilm-associated cells is essential to determine their efficacy across distinct physiological states relevant to infection. Bacterial time-kill analyses demonstrated synergistic activity between the primary active metabolite of erdosteine, MET-1 (10mg/L), and tobramycin against planktonic cultures of the MDR *P. aeruginosa* strain RP73, with combination therapy resulting in significant reductions in viable cell counts when combined with tobramycin at 1x and 4x MIC, respectively ($P < 0.05$). Whilst synergistic activity was also seen in planktonic cultures of the laboratory strain PA01, synergistic activity of the combination was only observed at 4 hours compared to tobramycin alone ($P < 0.05$). Significantly the potentiation of

tobramycin against planktonic cultures occurred despite MET-1 exhibiting no intrinsic antibacterial activity, as confirmed by MIC assays showing no reduction in bacterial metabolic activity at the highest soluble concentration tested (1024mg/L). No interaction was observed between MET-1 and tobramycin at sub-MIC concentrations, suggesting that the potentiating effects of MET-1 are restricted to bactericidal concentrations of tobramycin. The redox-active nature of MET-1 may suggest that redox-dependent processes may contribute to its interaction with tobramycin, as bacterial redox state and metabolic activity are known to influence antibiotic efficacy and cellular susceptibility (38).

A significant issue associated with the treatment of chronic *P. aeruginosa* is the propensity for *P. aeruginosa* to form biofilms. As biofilms mature, they transition from a temporary layer of surface-attached bacteria into a highly organised, complex and resilient three-dimensional structures which can impede antibiotic penetration, leading to increased resistance to antimicrobial therapy and necessitating higher doses that may cause renal and hepatic toxicity (39–41). Combination with 10mg/L MET-1 demonstrated a significant reduction in the Log IC50 of tobramycin in mature biofilms for both strains of *P. aeruginosa*, although this was not seen in young (6 hour) or developing biofilms. A key difference between young biofilms is the lack of a defined three-dimensional architecture and reduced complex matrix structures (42), whilst older biofilms often exhibit increased cell density, nutrient and oxygen gradients, and enhanced defence mechanisms such as efflux pump systems and reduced metabolic activity (6, 43). Combined with an increase in negatively charged biofilm matrix components in mature biofilms, these changes promote electrostatic sequestration of cationic antibiotics, such as tobramycin, reducing their penetration across the biofilm and therapeutic efficacy (44). This finding was replicated in our own study, where we demonstrated a significant increase in the IC50 of tobramycin in mature biofilms of RP73 and PA01 compared to young biofilms. The demonstration of antibiotic potentiating activity of MET-1 in mature, but not young or developing biofilms, is consistent with the hypothesis that MET-1 can enhance antibiotic penetration by breaking disulphide bonds that support the biofilm architecture via its free thiol group that can break disulphide bonds of mucus glycoproteins (5). This is supported by the identification that combination of tobramycin with 5 and 10mg/L MET-1 reduced the tobramycin IC50s in mature biofilms (24 and 48 hours) to levels lower than those seen in younger biofilms (6 hours) for both RP73 (IC50: Veh 6hrs: 25.16mg/L, + 10mg/L MET-1 at 48hrs: 4.80mg/L) and PA01 (IC50: Veh 6hrs: 4.57mg/L, + 10mg/L MET-1 at 48hrs: 1.82mg/L) which are less affected by impaired drug penetration. The lack of potentiation in younger biofilms may reflect the limited development of complex matrix structures that could be targeted by MET-1. Whilst future work quantifying antibiotic penetration using dye incorporation assays could be utilised to validate this hypothesis, this data highlights a significant therapeutic benefit for improving antibiotic penetration into biofilm-resident bacteria in the lungs of patients with chronic *P. aeruginosa* infections.

Extending from the *in vitro* analysis of MET-1 combination therapy with tobramycin we utilised a chronic mouse model of pulmonary infection with *P. aeruginosa*. For the treatment of respiratory diseases such as CB and COPD, the human dose regime is 300mg twice daily (19), we therefore calculated the mouse equivalent dose of 100mg once daily and treated animals for 10 days via oral gavage in line with the clinically approved prescription of erdosteine. Animals were also dosed with tobramycin that was either

sub-threshold, or associated with complete clearance (40 or 160mg/kg) as previously reported (32). In our studies, 160mg/kg completely cleared the infection, whilst monotherapy with either 100mg/kg erdosteine or 40mg/kg tobramycin failed to demonstrate any significant reduction in pulmonary bacterial load. However, combination of 100mg/kg erdosteine with 40mg/kg tobramycin demonstrated a significant reduction in bacterial titres 10 days post infection compared to vehicle treated controls. These results are consistent with previous clinical trials that demonstrated adjunct erdosteine therapy increased sputum β-lactam concentrations, resulting in faster symptom resolution in patients with CB (26). Furthermore, a systematic review and meta-analysis of seven RCTs in patients with stable or exacerbated CB/COPD confirmed that erdosteine plus antibiotics is more effective than antibiotics alone in treating acute infective exacerbations (27).

Interestingly, our *in vitro* studies demonstrate that the occurrence of MET-1 mediated potentiation of antibiotic activity occurred at tobramycin:MET-1 ratios of 2:5, with most clear responses observed at ratios of 8:5. In our *in vivo* studies, the tobramycin:erdosteine ratio was 1:10, 2:5 and 8:5 for 10, 40 and 160mg/kg tobramycin, respectively. Whilst further work is required to confirm the most appropriate dosing regimen for the combination, the lack of potentiation seen by erdosteine with 10mg/kg tobramycin (1:10) (data not shown) in our studies, combined with clinical trial data showing enhanced clearance at ratios 5:3 (26), suggests that combination therapy may require a minimum therapeutic ratio where antibiotic dose exceeds the erdosteine dose when developing future clinical trials.

In conclusion, our *in vitro* and *in vivo* analyses, alongside existing clinical data demonstrating the augmented antimicrobial activity of antibiotics when used in combination with erdosteine and its excellent safety profile, highlight the therapeutic potential of erdosteine. Adjunct therapy with erdosteine may therefore present a capacity to reduce both the dose and duration of antibiotic treatment in chronic *P. aeruginosa* infections or during acute infective PEx. This has the potential to provide significant improvements in patient care, clinical outcomes and reduced burden of long-term antimicrobial therapies highlighted as a key deliverable by the recent Jenny Lind Alliance priority setting exercise for patients with CF.

Declarations

Author Contributions: RTA and CPP were involved in the conceptualisation of the aims and goals of the project. BR, DG, MR, CC and AB were involved in the development of methodology, data curation and investigation; BR and RTA completed the formal analysis of the data; RTA and CPP were responsible for the acquisition of the financial support required for this project. BR and CC were involved in the investigation; RTA was responsible for the provision of resources and project administration; RTA and CPP were responsible for the supervision of the research activity; BR and RTA wrote the original draft, whilst CPP, CC and AB contributed to the review and editing of the manuscript.

Funding: This research was supported by an MRC doctoral training grant award to Richard Amison for Bailey Ramsden. Funding for the *in vivo* experiments was provided by Edmond Pharma, Italy to the San

Raffaele Institute, Milan.

Data availability statement: The data presented in this study are available on request from the corresponding authors.

Acknowledgements: The authors would like to thank B. Tümmler (Hannover Medical School, Hannover, Germany) for supplying the *P. aeruginosa* strain from a CF patient. We thank I. De Fino for technical support.

Conflicts of Interest

CPP acts as a Consultant to Edmond Pharma who developed and manufactures erdosteine**.**

References

1. Hirschmann JV (2000) Do Bacteria Cause Exacerbations of COPD? Chest [Internet]. Jul 1 [cited 2026 Mar 3];118(1):193–203. Available from: https://doi.org/10.1093/infdis/137.4.377
2. Ritchie AI, Wedzicha JA, Definition Causes, Pathogenesis, and Consequences of Chronic Obstructive Pulmonary Disease Exacerbations. Clin Chest Med [Internet]. 2020 Sep 1 [cited 2025 Feb 7];41(3):421–38. Available from: https://pubmed.ncbi.nlm.nih.gov/32800196/
3. Stanford GE, Dave K, Simmonds NJ Pulmonary Exacerbations in Adults With Cystic Fibrosis: A Grown-up Issue in a Changing Cystic Fibrosis Landscape. Chest [Internet]. 2020 Jan 1 [cited 2025 Feb 7];159(1):93. Available from: https://pmc.ncbi.nlm.nih.gov/articles/PMC7502225/
4. Wedzicha JA, Seemungal TA (2007) COPD exacerbations: defining their cause and prevention. Lancet (London, England) [Internet]. Sep 1 [cited 2025 Feb 10];370(9589):786–96. Available from: https://pubmed.ncbi.nlm.nih.gov/17765528/
5. Hall-Stoodley L, McCoy KS (2022) Biofilm aggregates and the host airway-microbial interface. Front Cell Infect Microbiol [Internet]. Aug 23 [cited 2026 Mar 3];12. Available from: https://pubmed.ncbi.nlm.nih.gov/36081767/
6. Wu H, Moser C, Wang HZ, Høiby N, Song ZJ Strategies for combating bacterial biofilm infections. Int J Oral Sci [Internet]. 2015 Mar 23 [cited 2026 Mar 3];7(1):1–7. Available from: https://pubmed.ncbi.nlm.nih.gov/25504208/
7. Ananth S, Adeoti AO, Ray A, Middleton PG, Ekkelenkamp M, Thee S et al Healthcare worker views on antimicrobial resistance in chronic respiratory disease. Antimicrob Resist Infect Control [Internet]. 2025 Dec 1 [cited 2026 Mar 3];14(1). Available from: https://pubmed.ncbi.nlm.nih.gov/39844291/
8. Pea C, Cabot G, Gómez-Zorrilla S, Zamorano L, Ocampo-Sosa A, Murillas J et al (2015) Influence of virulence genotype and resistance profile in the mortality of Pseudomonas aeruginosa bloodstream infections. Clin Infect Dis [Internet]. Feb 15 [cited 2022 Dec 9];60(4):539–48. Available from: https://pubmed.ncbi.nlm.nih.gov/25378459/

9. Walkty A, Lagace-Wiens P, Adam H, Baxter M, Karlowsky J, Mulvey MR et al (2017) Antimicrobial susceptibility of 2906 Pseudomonasaeruginosa clinical isolates obtained from patients in Canadian hospitals over a period of 8 years: Results of the Canadian Ward surveillance study (CANWARD), 2008–2015. Diagn Microbiol Infect Dis [Internet]. Jan 1 [cited 2022 Dec 9];87(1):60–3. Available from: https://pubmed.ncbi.nlm.nih.gov/28336136/
10. Sader HS, Castanheira M, Duncan LR, Flamm RK Antimicrobial Susceptibility of Enterobacteriaceae and Pseudomonas aeruginosa Isolates from United States Medical Centers Stratified by Infection Type: Results from the International Network for Optimal Resistance Monitoring (INFORM) Surveillance Program, 2015–2016. Diagn Microbiol Infect Dis [Internet]. 2018 Sep 1 [cited 2022 Dec 9];92(1):69–74. Available from: https://pubmed.ncbi.nlm.nih.gov/29789189/
11. Shaikh N, Lee A, Charma S, Cosgriff R, Carr S UK Cystic Fibrosis Registry 2020 Annual Data Report UK Cystic Fibrosis Registry 2020 Annual Data Report. 2021 [cited 2022 Dec 8];(3). Available from: https://www.cysticfibrosis.org.uk/sites/default/files/2022-03/2020 Annual data report - Version 3.pdf
12. Moretti M, Marchioni CF (2007) An overview of erdosteine antioxidant activity in experimental research. Pharmacol Res [Internet]. Apr 1 [cited 2026 Mar 3];55(4):249–54. Available from: https://www.sciencedirect.com/science/article/abs/pii/S1043661806002192?via%3Dihub
13. Cazzola M, Page C, Rogliani P, Calzetta L, Matera MG Multifaceted Beneficial Effects of Erdosteine: More than a Mucolytic Agent. Drugs [Internet]. 2020 Nov 1 [cited 2026 Mar 3];80(17):1799–809. Available from: https://link.springer.com/article/10.1007/s40265-020-01412-x
14. Santus P, Strizzi S, Danzo F, Biasin M, Saulle I, Vanetti C et al (2076) Antiviral Effect of Erdosteine in Cells Infected with Human Respiratory Viruses. Pathog 2025, Vol 14, [Internet]. 2025 Apr 14 [cited 2026 Mar 30];14(4). Available from: https://www.mdpi.com/-0817/14/4/388
15. Aubier M, Berdah L (1999) Multicenter, controlled, double-blind study of the efficacy and tolerance of Vectrine (erdostein) versus placebo in the treatment of stabilized chronic bronchitis with hypersecretion. Rev Mal Respir 16(4):521–528
16. Moretti M, Bottrighi P, Dallari R, Da Porto R, Dolcetti A, Grandi P et al (2005) The effect of long-term treatment with erdosteine on chronic obstructive pulmonary disease: the EQUALIFE Study. Drugs Exp Clin Res 31:31–44
17. Crisafulli E, Coletti O, Costi S, Zanasi E, Lorenzi C, Lucic S et al (2007) Effectiveness of erdosteine in elderly patients with bronchiectasis and hypersecretion: A 15-day, prospective, parallel, open-label, pilot study. Clin Ther [Internet]. Sep [cited 2026 Mar 4];29(9):2001–9. Available from: https://pubmed.ncbi.nlm.nih.gov/18035199/
18. Moretti M, Fagnani S Erdosteine reduces inflammation and time to first exacerbation postdischarge in hospitalized patients with AECOPD. Int J Chron Obstruct Pulmon Dis [Internet]. 2015 Oct 28 [cited 2026 Mar 3];10(1):2319–25. Available from: https://pubmed.ncbi.nlm.nih.gov/26604731/
19. Dal Negro RW, Wedzicha JA, Iversen M, Fontana G, Page C, Cicero AF et al (2017) Effect of erdosteine on the rate and duration of COPD exacerbations: the RESTORE study. Eur Respir J

[Internet]. Oct 1 [cited 2026 Mar 3];50(4):1700711. Available from: https://pmc.ncbi.nlm.nih.gov/articles/PMC5678897/

20. Calverley PMA, Page C, Dal Negro RW, Fontana G, Cazzola M, Cicero AF et al Effect of Erdosteine on COPD Exacerbations in COPD Patients with Moderate Airflow Limitation. Int J Chron Obstruct Pulmon Dis [Internet]. 2019 [cited 2026 Mar 3];14:2733–44. Available from: https://pubmed.ncbi.nlm.nih.gov/31819405/
21. Zatloukal J, Page C, Brat K, Svoboda M, Voláková E, Plutinský M et al Effect of Treatment with Mucoactive Drugs on COPD Exacerbations During 5 years of Follow-up in the Czech Republic: A Real-World Study. Lung [Internet]. 2025 Dec 1 [cited 2026 Mar 30];203(1). Available from: https://pubmed.ncbi.nlm.nih.gov/40327168/
22. Dal Negro R, Pozzi E, Cella SG, Erdosteine Drug exhibiting polypharmacy for the treatment of respiratory diseases. Pulm Pharmacol Ther [Internet]. 2018 Dec 1 [cited 2026 Mar 3];53:80–5. Available from: https://www.sciencedirect.com/science/article/abs/pii/S1094553918301883?via%3Dihub
23. Braga PC, Zuccotti T, Dal Sasso M (2001) Bacterial adhesiveness: effects of the SH metabolite of erdosteine (mucoactive drug) plus clarithromycin versus clarithromycin alone. Chemotherapy [Internet]. [cited 2026 Mar 3];47(3):208–14. Available from: https://pubmed.ncbi.nlm.nih.gov/11306790/
24. Braga PC, Dal Sasso M, Sala MT, Gianelle V Effects of erdosteine and its metabolites on bacterial adhesiveness. Arzneimittelforschung [Internet]. 1999 [cited 2026 Mar 3];49(4):344–50. Available from: https://pubmed.ncbi.nlm.nih.gov/10337454/
25. Pani A, Lucini V, Dugnani S, Scaglione F Erdosteine enhances antibiotic activity against bacteria within biofilm. Int J Antimicrob Agents [Internet]. 2022 Mar 1 [cited 2026 Mar 3];59(3). Available from: https://pubmed.ncbi.nlm.nih.gov/35051561/
26. Ricevuti G, Mazzone A, Uccelli E, Gazzani G, Fregnan GB (1988) Influence of erdosteine, a mucolytic agent, on amoxycillin penetration into sputum in patients with an infective exacerbation of chronic bronchitis. Thorax [Internet]. [cited 2026 Mar 3];43(8):585–90. Available from: https://pubmed.ncbi.nlm.nih.gov/3051508/
27. Rogliani P, Matera MG, Page C, Puxeddu E, Cazzola M, Calzetta L Efficacy and safety profile of mucolytic/antioxidant agents in chronic obstructive pulmonary disease: a comparative analysis across erdosteine, carbocysteine, and N-acetylcysteine. Respir Res 2019 201 [Internet]. 2019 May 27 [cited 2026 Mar 3];20(1):104-. Available from: https://link.springer.com/article/10.1186/s12931-019-1078-y
28. Jeukens J, Boyle B, Bianconi I, Kukavica-Ibrulj I, Tümmler B, Bragonzi A et al Complete Genome Sequence of Persistent Cystic Fibrosis Isolate Pseudomonas aeruginosa Strain RP73. Genome Announc [Internet]. 2013 Jan [cited 2016 Feb 5];1(4). Available from: http://www.pubmedcentral.nih.gov/articlerender.fcgi?artid=3731849&tool=pmcentrez&rendertype=abstract

29. Stover CK, Pham XQ, Erwin AL, Mizoguchi SD, Warrener P, Hickey MJ et al (2000) Complete genome sequence of Pseudomonas aeruginosa PAO1, an opportunistic pathogen. Nature [Internet]. Aug 31 [cited 2018 Sep 23];406(6799):959–64. Available from: http://www.nature.com/articles/35023079
30. Ramsden B, Kelis AV, Faure ME, Page CP, Amison RT Synergistic Interactions Between the Quinolone-Derived Compound HT61 and Tobramycin Against a Range of Clinical Isolates of Pseudomonas aeruginosa In Vitro. Lung [Internet]. 2025 Dec 1 [cited 2026 Mar 3];203(1). Available from: https://pubmed.ncbi.nlm.nih.gov/41307567/
31. Amison RT, Faure ME, O'Shaughnessy BG, Bruce KD, Hu Y, Coates A et al (2020) The small quinolone derived compound HT61 enhances the effect of tobramycin against Pseudomonas aeruginosa in vitro and in vivo. Pulm Pharmacol Ther 61:101884
32. Cigana C, Ranucci S, Rossi A, De Fino I, Melessike M, Bragonzi A (2020) Antibiotic efficacy varies based on the infection model and treatment regimen for Pseudomonas aeruginosa. Eur Respir J [Internet]. Mar 1 [cited 2026 Mar 3];55(3). Available from: https://pubmed.ncbi.nlm.nih.gov/31624114/
33. Belley A, Neesham-Grenon E, Arhin FF, McKay GA, Parr TR, Moeck G Assessment by Time-Kill Methodology of the Synergistic Effects of Oritavancin in Combination with Other Antimicrobial Agents against Staphylococcus aureus. Antimicrob Agents Chemother [Internet]. 2008 Oct [cited 2023 Nov 6];52(10):3820. Available from: /pmc/articles/PMC2565878/
34. Calzetta L, Page C, Matera MG, Cazzola M, Rogliani P (2024) Drug-Drug Interactions and Synergy: From Pharmacological Models to Clinical Application. Pharmacol Rev 76(6):1159–1220
35. EUCAST Breakpoint tables for interpretation of MICs and zone diameters. Breakpoint tables for interpretation of MICs and zone diameters. Available from: https://eucast.org
36. Facchini M, De Fino I, Riva C, Bragonzi A (2014) Long term chronic Pseudomonas aeruginosa airway infection in mice. J Vis Exp [Internet]. Jan [cited 2015 Oct 16];(85). Available from: http://www.ncbi.nlm.nih.gov/pubmed/24686327
37. Staudinger BJ, Muller JF, Halldórsson S, Boles B, Angermeyer A, Nguyen D et al (2014) Conditions Associated with the Cystic Fibrosis Defect Promote Chronic Pseudomonas aeruginosa Infection. Am J Respir Crit Care Med [Internet]. Apr 1 [cited 2026 Mar 3];189(7):812. Available from: https://pmc.ncbi.nlm.nih.gov/articles/PMC4225830/
38. Tawiah PO, Sultana S, Dahl JU Unlocking Enhanced Efficacy of Aminoglycoside Antibiotics Against Pseudomonas aeruginosa. Microb Biotechnol [Internet]. 2025 Jun 1 [cited 2026 Mar 4];18(6):e70174. Available from: https://pmc.ncbi.nlm.nih.gov/articles/PMC12124998/
39. Nickel JC, Ruseska I, Wright JB, Costerton JW Tobramycin resistance of Pseudomonas aeruginosa cells growing as a biofilm on urinary catheter material. Antimicrob Agents Chemother [Internet]. 1985 [cited 2026 Mar 3];27(4):619–24. Available from: https://pubmed.ncbi.nlm.nih.gov/3923925/
40. Prayle A, Watson A, Fortnum H, Smyth A (2010) Side effects of aminoglycosides on the kidney, ear and balance in cystic fibrosis. Thorax [Internet]. Jul 1 [cited 2019 Feb 5];65(7):654–8. Available from: http://thorax.bmj.com/cgi/doi/10.1136/thx.2009.131532

41. Al-Aloul M, Miller H, Alapati S, Stockton PA, Ledson MJ, Walshaw MJ Renal impairment in cystic fibrosis patients due to repeated intravenous aminoglycoside use. Pediatr Pulmonol [Internet]. 2005 Jan [cited 2019 Feb 5];39(1):15–20. Available from: http://doi.wiley.com/10.1002/ppul.20138
42. Rather MA, Gupta K, Mandal M Microbial biofilm: formation, architecture, antibiotic resistance, and control strategies. Brazilian J Microbiol [Internet]. 2021 Dec 1 [cited 2026 Mar 4];52(4):1701. Available from: https://pmc.ncbi.nlm.nih.gov/articles/PMC8578483/
43. Fu J, Zhang Y, Lin S, Zhang W, Shu G, Lin J et al Strategies for Interfering With Bacterial Early Stage Biofilms. Front Microbiol [Internet]. 2021 Jun 8 [cited 2026 Mar 3];12:675843. Available from: https://pmc.ncbi.nlm.nih.gov/articles/PMC8217469/
44. Hatch RA, Schiller NL Alginate lyase promotes diffusion of aminoglycosides through the extracellular polysaccharide of mucoid Pseudomonas aeruginosa. Antimicrob Agents Chemother [Internet]. 1998 [cited 2026 Mar 3];42(4):974–7. Available from: https://pubmed.ncbi.nlm.nih.gov/9559826/

Tables

Table 1 is available in the Supplementary Files section.

Figures

Figure 1

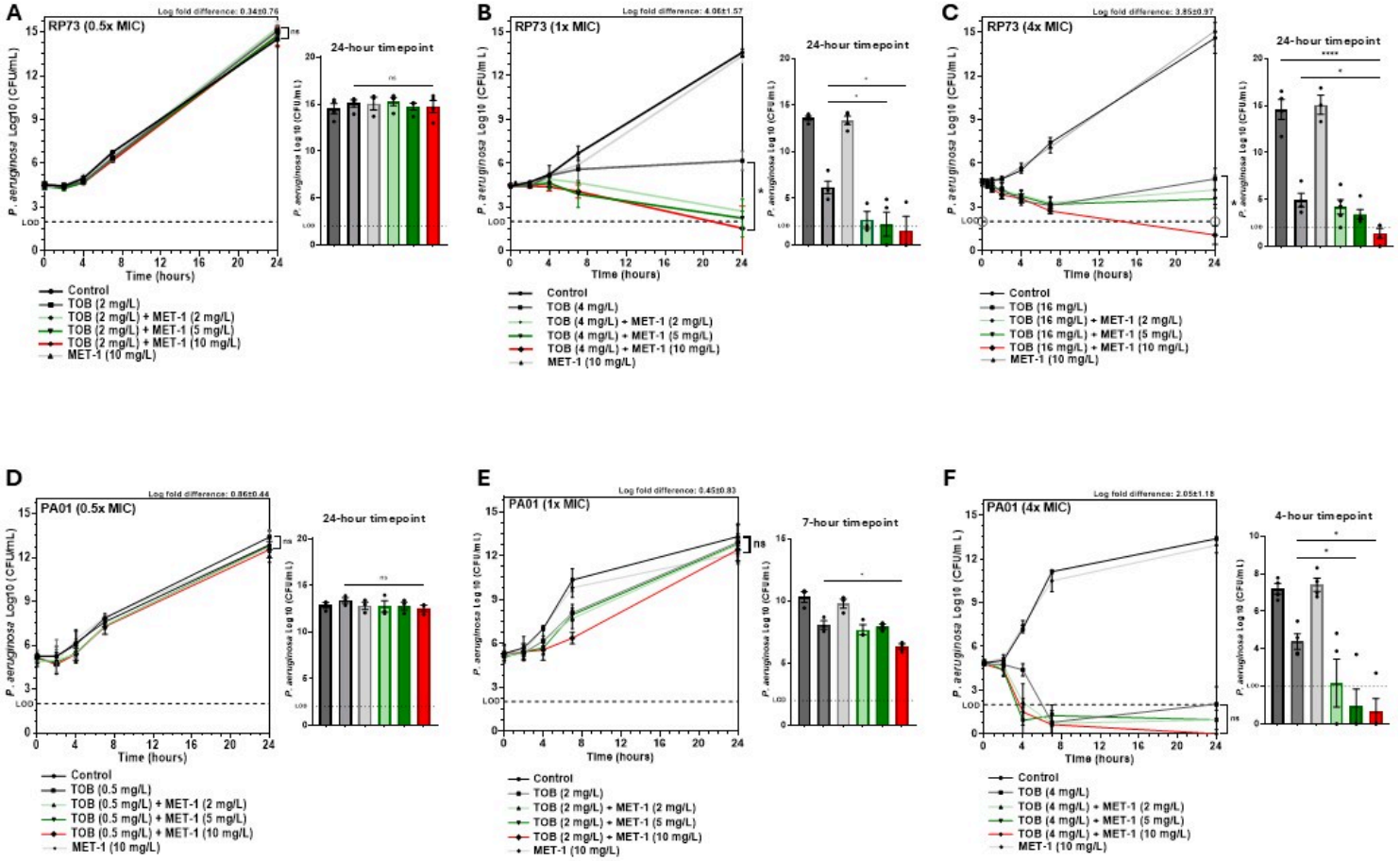


Figure 1

Bacterial time-kill analyses of RP73 and PA01 using tobramycin at concentrations 0.5x, 1x, and 4x the MIC. Tobramycin MICs were 4 mg/L and 1 mg/L for RP73 (**A-C**) and PA01 (**D-F**), respectively. Aliquots from the control, tobramycin monotherapy, MET-1 (10 mg/L) monotherapy and tobramycin in combination with 2 mg/L, 5 mg/L and 10 mg/L MET-1 were collected for enumeration at 0-, 2-, 4-, 7- and 24-hours post-treatment. Statistical significance of the drug interaction of the combination (tobramycin + MET-1 10 mg/L) compared to tobramycin monotherapy at 24 hours was determined using the BLUR model of synergy and indicated with a * ($P < 0.05$) or ns (not significant). Bar charts display the log-transformed cell counts at 24 hours (**A-D**), 7 hours (**E**) and 4 hours (**F**). Differences between tobramycin monotherapy and the three combinations were assessed using an ordinary one-way ANOVA followed by Tukey's test (ns, $P > 0.05$; * $P \leq 0.05$; ** $P \leq 0.01$; *** $P \leq 0.001$; and **** $P \leq 0.0001$). All significant differences between groups are indicated, where there was no significant difference between any group, only TOB vs TOB MET-1 combination at highest concentration (10 mg/L) is labelled ns. Limit of detection (LOD) is marked with a dotted line at Log2 cfu/mL. Data presented as mean ± SEM log cfu/mL, N = 3-5 per group.

Figure 2

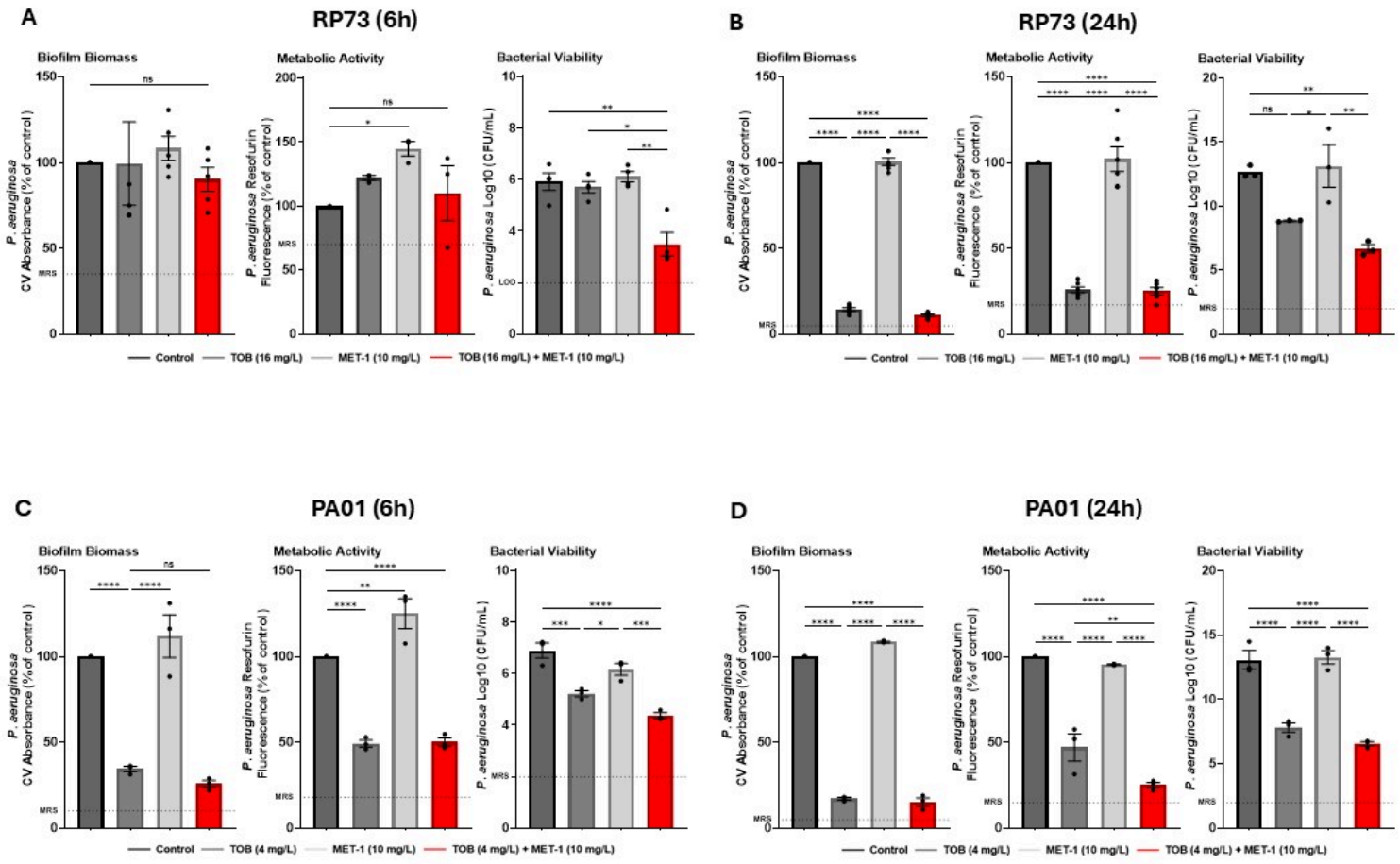


Figure 2

Effect of MET-1 on tobramycin activity in developing biofilms as measured by biofilm biomass, metabolic activity and bacterial viability of biofilm-associated cells. RP73 and PA01 biofilms were grown in the presence of vehicle, tobramycin at 4x MIC, MET-1 (10 mg/L), or tobramycin at 4x MIC in combination with either 2 mg/L, 5 mg/L or 10 mg/L MET-1. Tobramycin MICs were 4 mg/L and 1 mg/L for RP73 (**A+B**) and PA01 (**C+D**), respectively. Biofilms were assessed following 6 and 24 hours of incubation at 37°C under static conditions. Biofilm biomass was measured by crystal violet staining, metabolic activity through the formation of resorufin and bacterial content by quantification. Crystal violet and resorufin data are presented as percentage of control. Minimum reliable signal (MRS) as a percentage of control and limit of detection (LOD) is marked with a dotted line. Treatment groups were compared using an ordinary 1-way ANOVA followed by Tukey's multiple comparison test (ns, $P > 0.05$; * $P \leq 0.05$; ** $P \leq 0.01$; *** $P \leq 0.001$; and **** $P \leq 0.0001$). All significant differences between TOB and other treatments groups are indicated, where there were no significant differences, only TOB vs TOB-MET-1 combination at the highest concentration (10 mg/L) is labelled ns. Data presented as mean ± SEM, N = 3–5 per group.

Figure 3

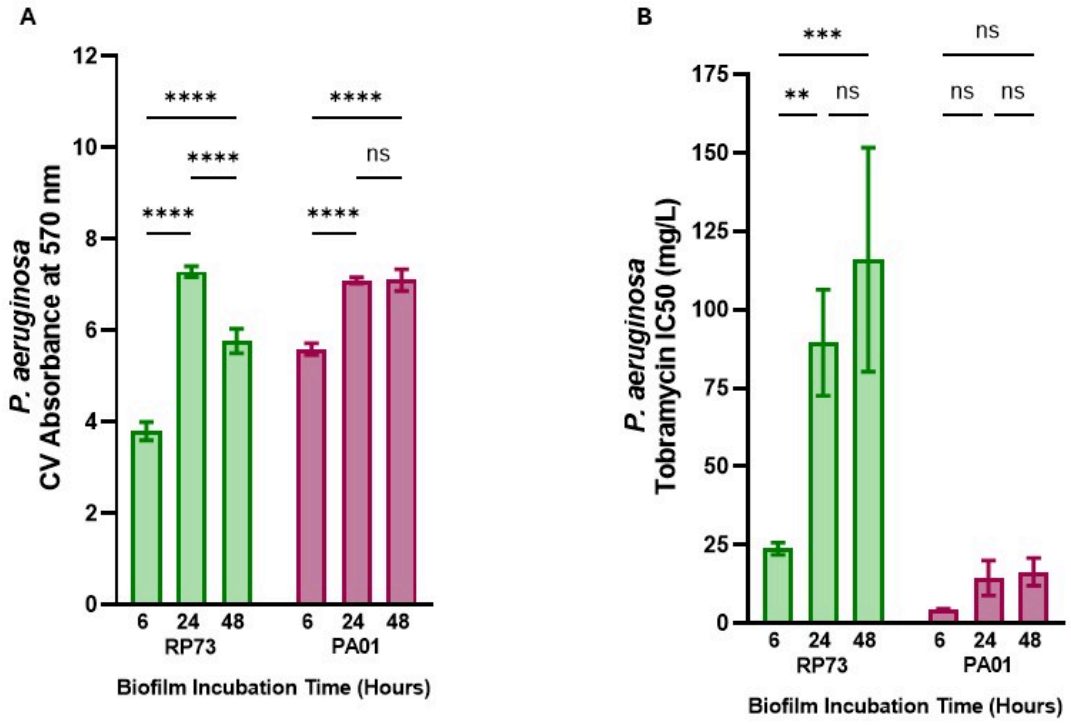


Figure 3

Mature biofilms are associated with increased biomass and reduced sensitivity to tobramycin. Biofilms were left to incubate for up to 48 hours and biomass quantified via measurement of crystal violet absorbance at 570nm (**A**). In additional studies, established biofilms were treated with tobramycin (0-800x MIC) at 6, 24 or 48 hrs and incubated for a further 24 hrs. Biomass was quantified via measurement of crystal violet absorbance at 570nm and IC50s for tobramycin calculated. Significant differences in biofilm biomass or metabolic activity after 6, 24 and 48 hours were determined using an ordinary two-way ANOVA followed by Tukey's test (ns, $P > 0.05$; * $P \leq 0.05$; ** $P \leq 0.01$; *** $P \leq 0.001$; and **** $P \leq 0.0001$). Minimum reliable signal (MRS) is marked with a dotted line.

Figure 4

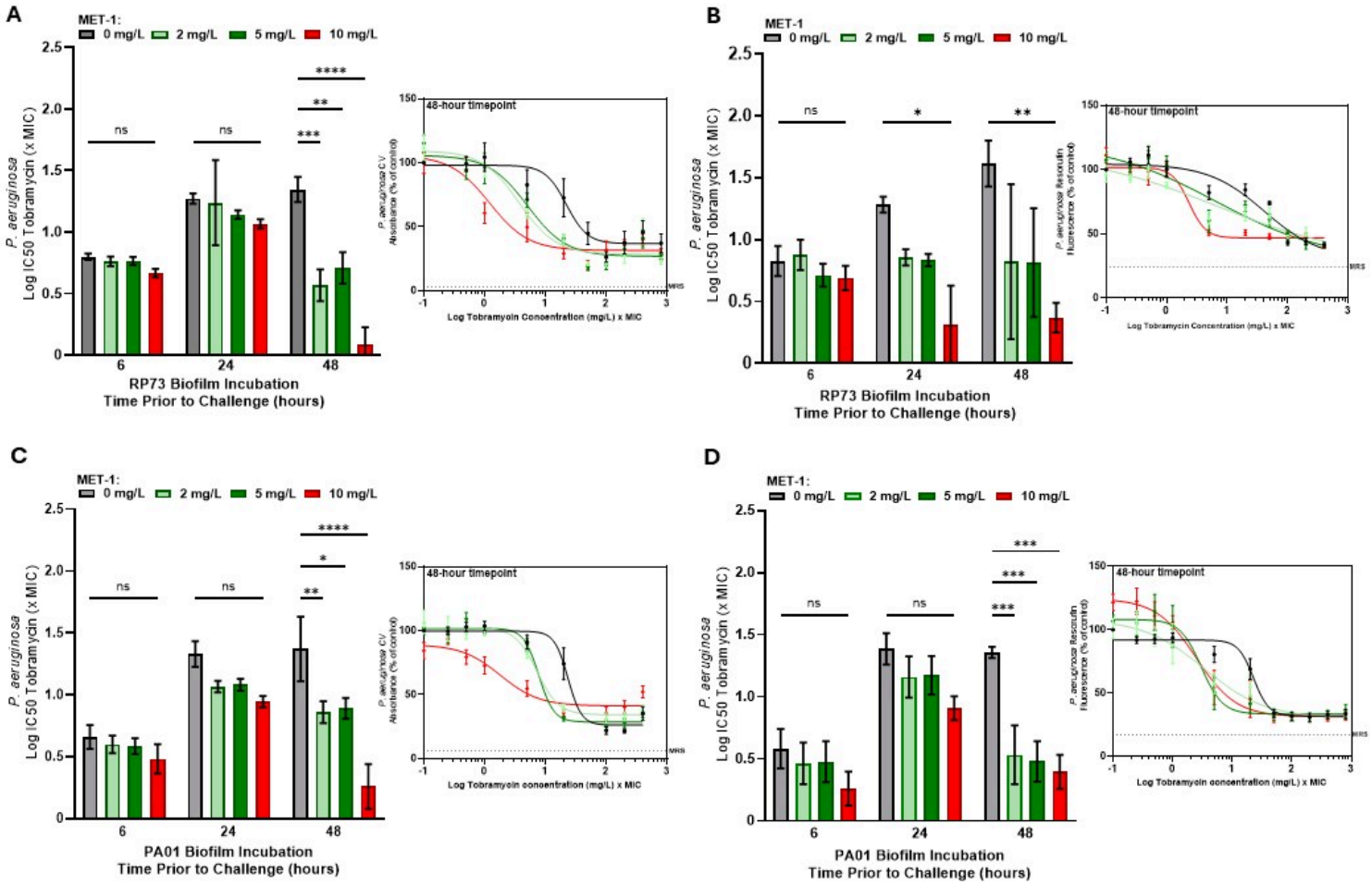


Figure 4

Effect of MET-1 on tobramycin activity in established biofilms as measured by biofilm biomass and metabolic activity. Schematics illustrating changes in biofilm biomass (**A & C**) and metabolic activity (**B & D**) of established biofilms of RP73 (**A & B**) and PA01 (**C & D**) treated with tobramycin 0-800x MIC either alone or in combination with 2 mg/L, 5 mg/L or 10 mg/L MET-1. Tobramycin MICs were 4 mg/L and 1 mg/L for RP73 and PA01, respectively. Following treatment at either 6, 24 or 48 hours, biofilms were left to incubate for a further 24 hours. Significant differences in biofilm biomass or metabolic activity after 6, 24 and 48 hours were determined using an ordinary two-way ANOVA followed by Tukey's test (ns, $P > 0.05$; * $P \leq 0.05$; ** $P \leq 0.01$; *** $P \leq 0.001$; and **** $P \leq 0.0001$). Minimum reliable signal (MRS) is marked with a dotted line.

Figure 5: MET1 augments tobramycin activity in a murine model of chronic *P.aeruginosa* infection

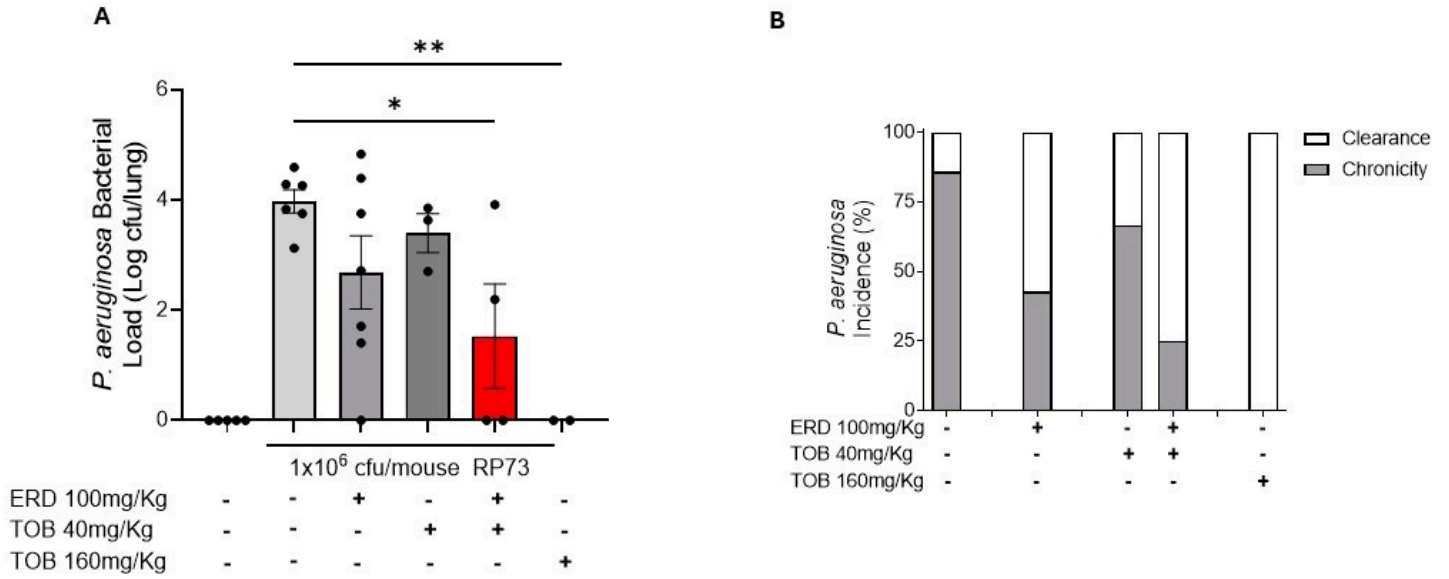


Figure 5

Effects of combination therapy of tobramycin and erdosteine in a murine model of chronic pulmonary infection with RP73. C57Bl/6 mice (aged 8-10 weeks) received intratracheal inoculation with 1x106 cfu/mouse RP73 embedded in agar beads. Animals received daily therapy with either vehicle or 40 mg/kg tobramycin *s.c.* in the presence or absence of 100 mg/kg erdosteine *p.o.* 160 mg/kg tobramycin monotherapy was also used as a positive control demonstrating complete eradication. Animals were monitored daily throughout the duration of the study. 10 days post infection, mice were killed, the lungs excised, homogenised and plated on tryptic soy agar to determine the bacterial burden (**A**), whilst data was also expressed as the percentage of animals clearing the pulmonary infection between each treatment group (**B**). A cut-off of 1000 cfu/lung was used to distinguish bacterial clearance from chronic colonisation N= 2-8 per group. Data was confirmed as normally distributed using the Shapiro-Wilks normality test and subsequently analysed using a one-way ANOVA followed by Sidaks multiple comparison post-test (* $P < 0.05$, ** $P < 0.01$).

Supplementary Files

This is a list of supplementary files associated with this preprint. Click to download.

- Table1.jpg
- SupplementaryFigure1.jpg